Progress In Electromagnetics Research Letters, Vol. 57, 117–123, 2015

Compact Four-Element Antenna Array Design for BeiDou Navigation Satellite System Applications

Jianxing Li[1, *], Hongyu Shi[1], Jianying Guo[1], and Anxue Zhang[1, 2]

Abstract—In this letter, a compact four-element microstrip patch antenna array for BeiDou navigation satellite system (BDS) operation at the B3 (1268 MHz) band is proposed. High permittivity dielectric substrate and slit-loaded microstrip patch are used to reduce the antenna element size down to 40 mm × 40 mm which implies an aperture size of only $\lambda_0/6 \times \lambda_0/6$ at the B3 band. The right-handed circularly polarized (RHCP) radiation is achieved by connecting two coaxial probes to a 0°–90° stripline hybrid. Four identical antenna elements are distributed with the same polarity and an inter-element separation of 80 mm ($\lambda_0/3$ at the B3 band). The overall size of the antenna array, including the stripline feeding network and supporting ground plane, is only 140 mm × 140 mm × 5.5 mm. A prototype was fabricated and measured to verify the design concept. Simulated and measured results will be presented and discussed, showing that the proposed BDS antenna array is suitable for BDS applications.

1. INTRODUCTION

Global navigation satellite systems (GNSS) receivers must operate efficiently under all environments to ensure robust and accurate acquisition of position, velocity and time (PVT) for aviation, maritime, and consumer electronics. Both commercial and military GNSS receivers are vulnerable to interfering signals, since signals from navigation satellites are at least 20 dB below the ambient noise floor [1]. Consequently, apart from wide bandwidth and multi-band GNSS antennas, adaptive antennas with sophisticated nulling and beamforming algorithms have been envisaged universally for GNSS applications [2]. Adaptive antennas with multi-element antenna arrays have capabilities to provide real-time adaptive nulling and beamforming to preserve satellite signals while suppressing all interfering signals [3]. Multi-element antenna arrays typically with an inter-element separation of half of the free space wavelength are usually rendered too large for small platforms. Certainly, reducing the inter-element separation could results in a much more compact antenna array. However, the antenna array may suffer strong mutual coupling between the individual antenna elements, affecting the resonant frequencies, return loss, and radiation patterns considerably. As a consequence, the nulling and beamforming performance of the adaptive antennas can be significantly deteriorated [4]. To date, a large number of multi-element antenna arrays with reduced size, acceptable radiation property, and reasonable inter-element isolation have been proposed [5–8]. Chinese BeiDou navigation satellite system (BDS) has already been providing services for the Asia-Pacific region. At present, only the BDS B3 signal (1268.52 ± 10.23 MHz) is modulated with the precision ranging code (P code) [9]. Therefore, it is desirable to develop and design compact multi-element antenna arrays for BDS B3 adaptive antenna applications. Unfortunately, most of the reported designs can operate merely at the GPS bands [5–7]. Zhou et al. proposed a tri-band proximity-fed GPS antenna using stacked substrates [5]. However, the antenna exhibits relatively high profile. A four-element spiral array using resistor terminations and ferrite beads was designed to operate from

Received 6 October 2015, Accepted 3 November 2015, Scheduled 11 November 2015

* Corresponding author: Jianxing Li (jianxingli.china@gmail.com).

[1] School of Electronic and Information Engineering, Xi'an Jiaotong University, Xi'an, Shaanxi 710049, China. [2] Beijing Center for Mathematics and Information Interdisciplinary Science (BCMIIS), Beijing 100048, China.

1100 to 1600 MHz [6]. Nonetheless, the loaded resistors compromise the radiation efficiency, and hence reduce the antenna gains. In [7], a dual-band proximity-fed GPS antenna was developed using high dielectric ceramic which may increase the antenna cost. Besides, these antennas also have much larger profiles [6, 7].

In this letter, we present a compact four-element antenna array operating at the BDS B3 band. High permittivity dielectric substrate and slit-loaded microstrip patch are used to minimize the antenna element size. Two coaxial probes with quadrature phase are employed to feed individual antenna elements and ensure right-handed circularly polarized (RHCP) radiation. The two coaxial probes are then connected to the outputs of a stripline 0°–90° hybrid to reduce feed complexity. In the following sections: Section 2 describes design considerations of the antenna element as well as the antenna array configuration; Section 3 presents and discusses the simulated and measured results; conclusions are finally drawn in Section 4.

2. ANTENNA ELEMENT AND ARRAY DESIGN

We start with the miniaturization of the antenna element in order to reduce the mutual coupling through increasing the physical separation between the individual antenna elements. Fig. 1(a) shows the geometry of the microstrip patch antenna element. The patch is printed on a 40 mm × 40 mm Taconic CER-10 substrate ($\tan\delta = 0.0035$) with high dielectric constant $\varepsilon_r = 10.3$ and thickness $h = 3.18$ mm to reduce the antenna element size, implying an aperture of only $\lambda_0/6 \times \lambda_0/6$, where λ_0 is the wavelength of the center frequency for BDS B3 band in the free space. Furthermore, we introduce the idea from [10] to etch two pairs of symmetric slits at each patch edge to lengthen the effective excited patch surface current path, and hence obtain the antenna element with reduced size. Two coaxial probes with quadrature phase located at A (x_p, 0) and B (0, y_p) are used to feed the antenna element, which will generate two orthogonal linearly polarized modes (TM_{10} and TM_{01}), and thus ensure RHCP radiation property. It

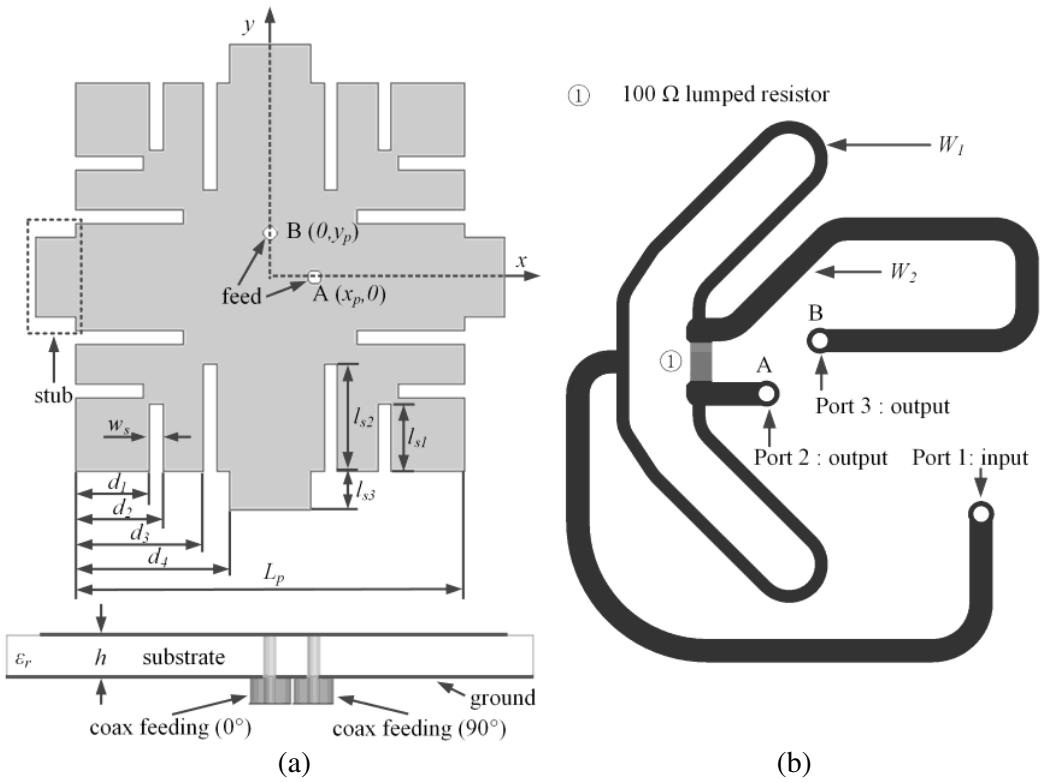

Figure 1. (a) Geometry of the microstrip patch antenna element. (b) Layout of the stripline 0°–90° hybrid.

is well known that the resonant frequency of the antenna element can be effected when placed in an antenna array. Therefore, four identical stubs are loaded at the center of patch edges, which can be trimmed conveniently to relocate the resonant frequencies for individual antenna elements during the fabrication process.

The probe-fed antenna element requires eight feeding ports and four 0°–90° hybrids when part of a four-element BDS antenna array, which is undesirable and expensive for a compact antenna array. Next, we proceeded to design a stripline 0°–90° hybrid to obtain RHCP radiation and reduce the feed complexity simultaneously. Fig. 1(b) shows the layout of the 0°–90° stripline hybrid. The hybrid is realized using striplines printed within a low cost F4B substrate with dielectric constant 2.65 and thickness 2.0 mm. The stripline hybrid output ports (A, B) are connected to the corresponding feeding probes (A, B) indicated in Fig. 1(a). To obtain desired power splitting and stable quadrature phase outputs, a cascade of 3-dB Wilkinson power divider and a 90° phase shifter with different lengths of striplines are employed. When compared to the microstrip feeding networks [5–7], the stripline one could further decrease the mutual coupling between the patch antenna and the feeding network.

The ANSYS-Ansoft high-frequency structure simulator (HFSS) was used to design and optimize the geometrical parameters. The optimal parameters are determined as follows: $L_p = 29.0$ mm, $d_1 = 5.5$ mm, $d_2 = 6.5$ mm, $d_3 = 9.5$ mm, $d_4 = 11.5$ mm, $l_{s1} = 5.0$ mm, $l_{s2} = 8.0$ mm, $l_{s3} = 3.0$ mm, $w_s = 1.0$ mm, $x_p = 3.3$ mm, $y_p = 3.3$ mm, $W_1 = 0.77$ mm, and $W_2 = 1.43$ mm.

Then, four identical antenna elements are distributed with the same polarity to construct a square array, which has all-azimuth scanning capability and compactness characteristic [11]. As shown in Fig. 2, the inter-element separation is determined to be 80 mm, approximately $\lambda_0/3$. Also, a square ground plane with finite size 140 mm × 140 mm is used to support the four-element BDS antenna array both in the simulations and measurements.

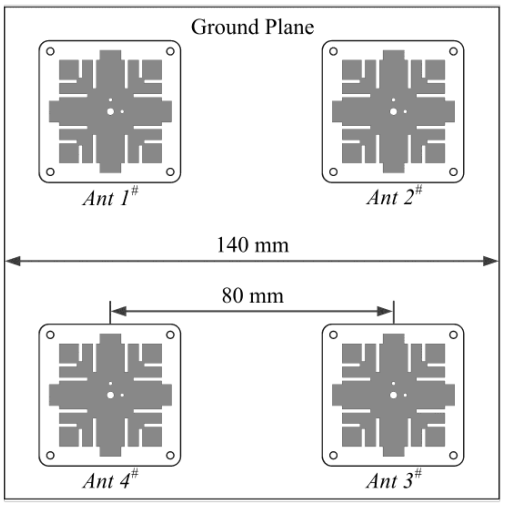

Figure 2. Configuration of the four-element BDS antenna array.

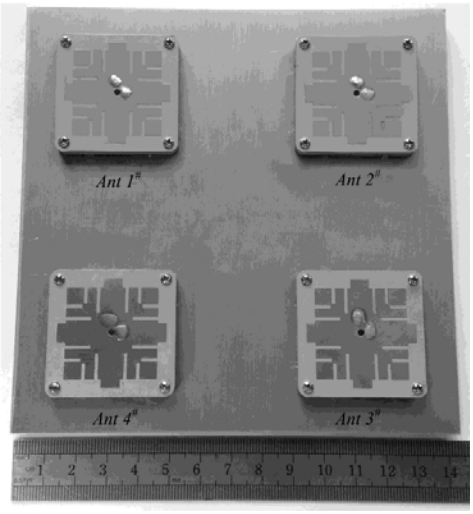

Figure 3. Fabricated antenna element and assembled antenna array.

3. RESULTS AND DISCUSSIONS

Figure 3 shows the fabricated and assembled four-element BDS antenna array, where the antenna elements and 0°–90° stripline hybrids are integrated together. Each antenna element is fastened on the ground plane using four screws. A 50-Ω SMP connector is used at each antenna element input port, and a 100-Ω surface mount chip resistor is soldered at each stripline hybrid.

The S-parameters of the fabricated antenna array are measured with an Agilent E8363B network analyzer. Fig. 4 presents the simulated and measured S-parameters. Although the measured and simulated results are slightly different, both of them show that the reflection coefficients are below

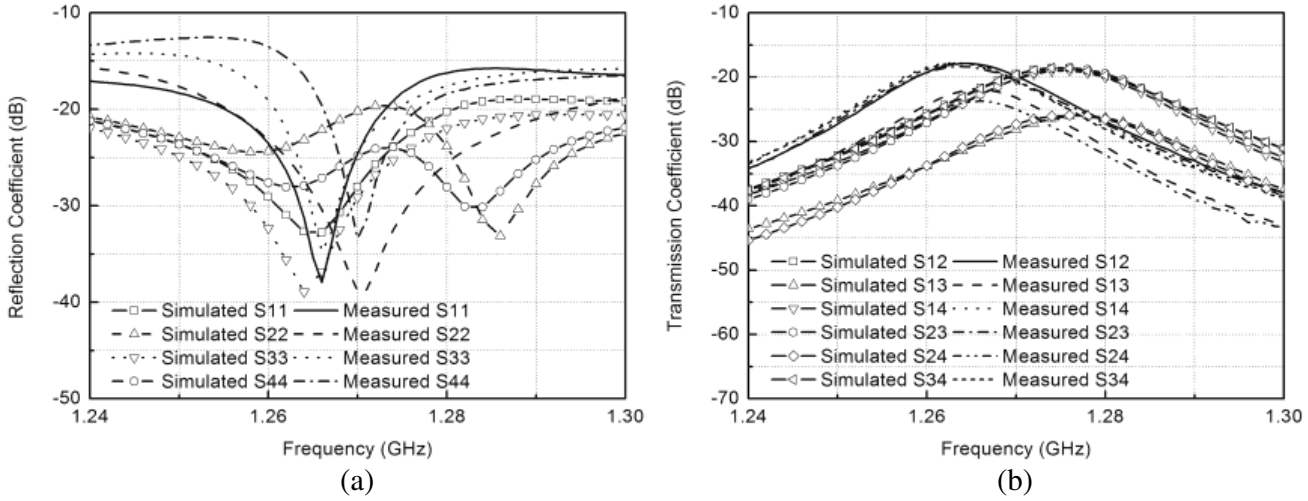

Figure 4. Simulated and measured S-parameters. (a) Reflection coefficient. (b) Transmission coefficient.

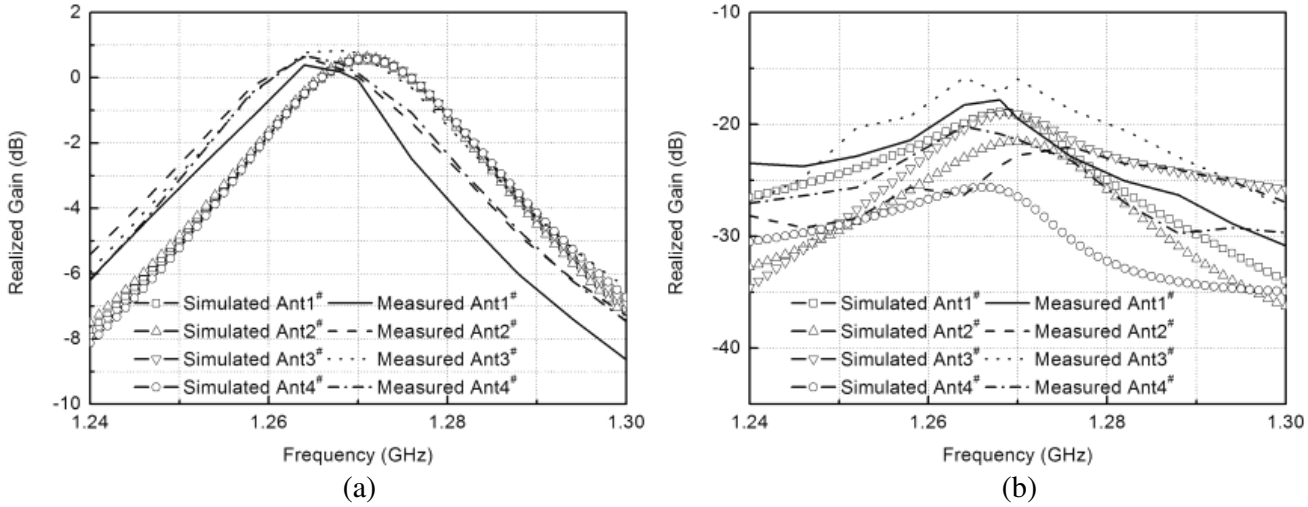

Figure 5. Simulated and measured broadside realized gain. (a) RHCP. (b) LHCP.

-15 dB (corresponding to VSWR < 1.5) over the BDS B3 band, which is fairly enough for satellite signals reception. Discrepancies are most likely due to fabrication inaccuracies and residual air gaps between the antenna elements and the feeding networks, and the substrates may not have totally uniform dielectric constant. Furthermore, it can be observed from Fig. 4(b) that reasonable isolation between the individual elements is achieved, which maintains above 18 dB across the BDS B3 band. It implies that it would have almost no effect on the performance of adaptive antennas adopting the space-time adaptive processing (STAP) algorithms [12].

Figure 5 shows the simulated and measured RHCP and left-handed CP (LHCP) gains in the broadside directions ($\theta = 0^\circ$) for the individual antenna elements. Reasonable agreement between the simulated results and measured ones can be observed. The RHCP-to-LHCP isolation is above 17 dB over the BDS B3 band for all the antenna elements, implying excellent polarization purity.

The simulated and measured AR in the broadside direction and the simulated radiation efficiency are given in Fig. 6. We can see from Fig. 6(a) that both the simulations and measurements show that the broadside AR is kept less than 3.0 dB at the B3 band for all the antenna elements. It demonstrates

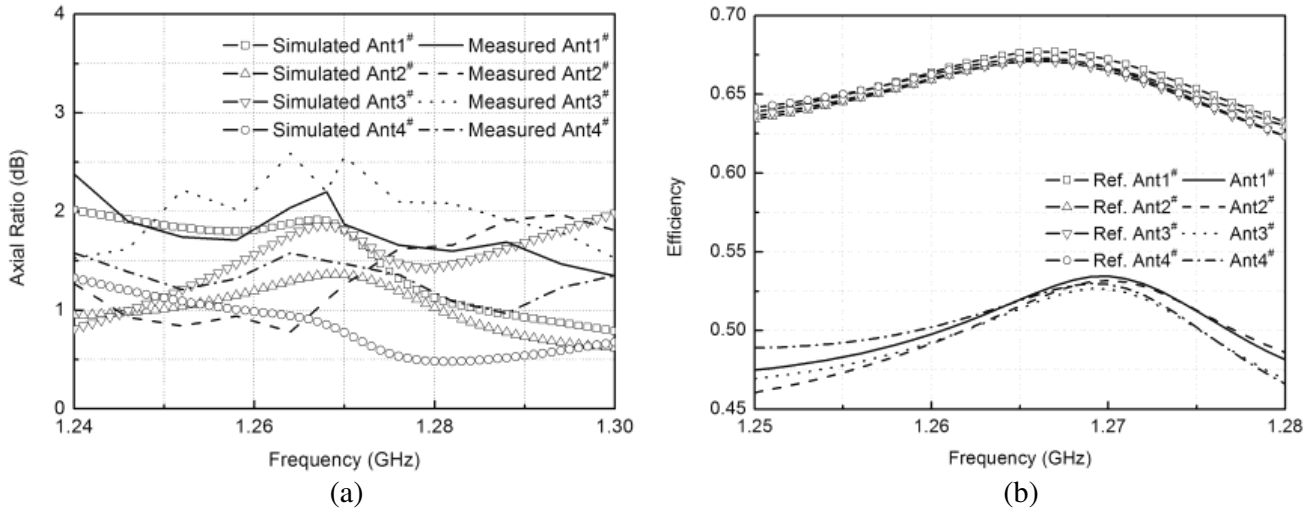

Figure 6. (a) Simulated and measured broadside axial ratio. (b) Simulated radiation efficiency.

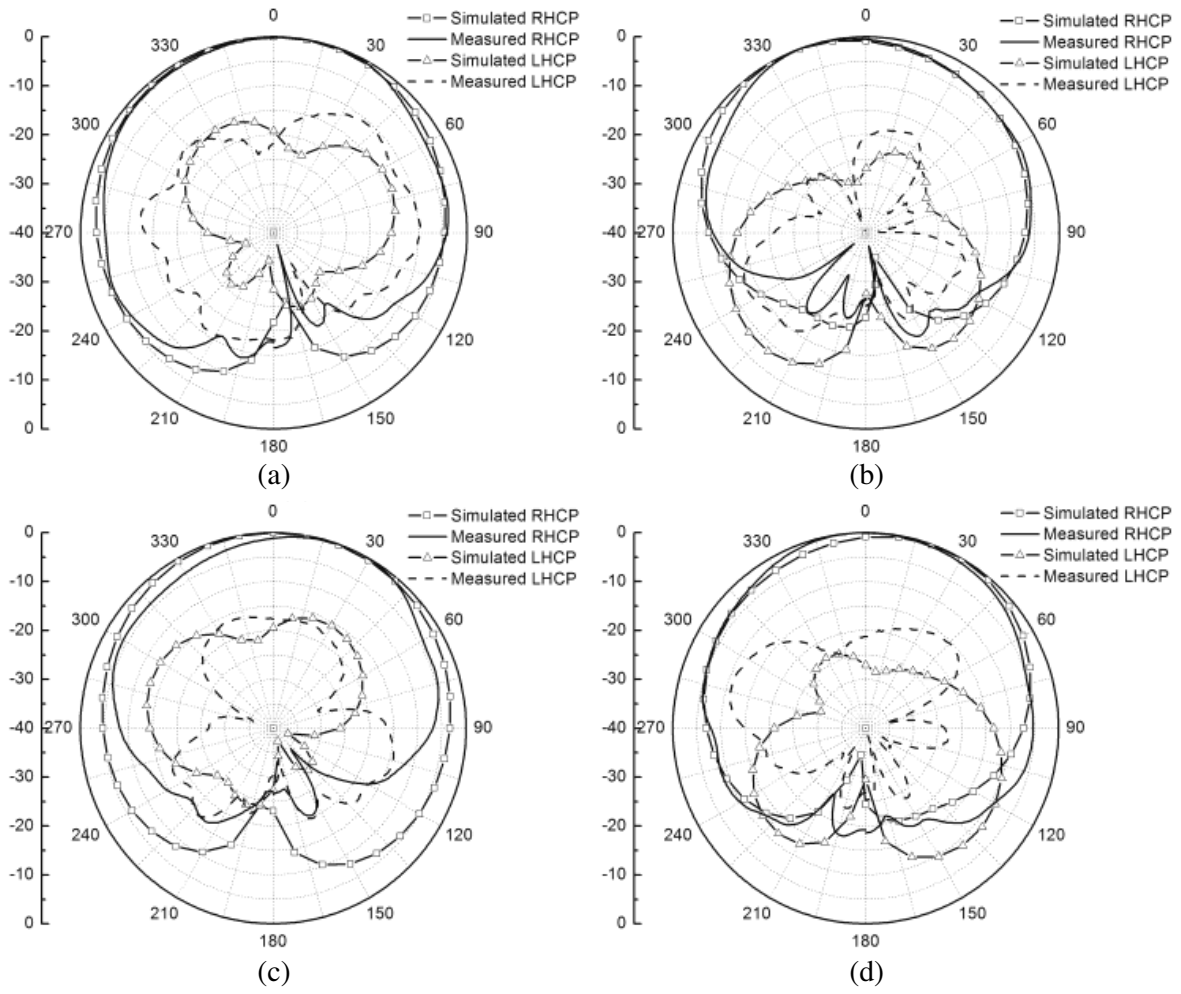

Figure 7. Simulated and measured radiation patterns. (a) *Ant1*#. (b) *Ant2*#. (c) *Ant3*#. (d) *Ant4*#.

a good RHCP property. As shown in Fig. 6(b), the simulations indicate that radiation efficiency of around 67% is achieved in the reference design [8], resulting from the high-loss dielectric material and the low-thickness substrate. However, due to the reduced aperture size and the meandered patch, the radiation efficiency for the proposed antenna array dropped to around 52%. Since this is a BDS receiver antenna array, the fact that radiation efficiency is not very high is not a major concern.

It is well known that mutual coupling between closely distributed antenna elements often affects radiation patterns of the antenna elements. The radiation patterns for the individual antenna elements placed in the proposed antenna array were further measured in an anechoic chamber. In the measurement, the position of the antenna array was changed accordingly to make sure that the center of the antenna element under test was aligned with the center of the transmitting antenna. Fig. 7 presents the normalized simulated and measured E-plane ($\varphi = 0°$, θ: $0° \sim 360°$) radiation patterns at the center frequency of the BDS B3 band, which shows the measurements are in good agreement with the simulations. It should be noticed that these patterns are tilted towards different but known angular region, and not completely symmetric, as a result of the mutual coupling between the individual antenna elements and the finite ground plane scattering. However, wide sky coverage and reasonable polarization isolation can still be preserved. We further note that the measured peak gain for $Ant1^{\#}$, $Ant2^{\#}$, $Ant3^{\#}$, and $Ant4^{\#}$ is 1.29 dBic, 1.36 dBic, 1.40 dBic, and 1.41 dBic, respectively. The measured AR at zenith is 2.2 dB for $Ant1^{\#}$, 1.1 dB for $Ant2^{\#}$, 2.2 dB for $Ant3^{\#}$, and 1.5 dB for $Ant4^{\#}$, implying good RHCP performance.

4. CONCLUSIONS

This letter proposes a compact four-element antenna array for BDS B3 applications. High permittivity dielectric substrate and slit-loaded microstrip patch are used to reduce the antenna element size. The footprint of the antenna element with the feeding network is only $\lambda_0/6 \times \lambda_0/6$ at the BDS B3 band. A 0°–90° stripline hybrid is introduced to ensure RHCP radiation property. A square array fulfilled with four identical antenna elements distributed in the same polarity is fabricated and assembled. The inter-element separation is 80 mm ($\lambda_0/3$ at the B3 band). Experimental results show that reasonable mutual coupling between antenna elements has been obtained, maintaining more than 18 dB over the whole BDS B3 band. The overall size of the proposed antenna array with the feeding networks and the ground plane is 140 mm × 140 mm × 5.5 mm. Although the radiation patterns of the antenna elements are tilted toward different angular region due to the mutual coupling and the finite ground plane scattering, wide sky coverage and good polarization purity are still achieved at the BDS B3 band. Therefore, the compact aperture size and good radiation performance makes the proposed antenna array attractive for small BDS platforms.

REFERENCES

1. Kaplan, E. D. and C. J. Hegarty, *Understanding GPS: Principles and Applications*, 2nd Edition, Artech House, Boston, MA, 2006.
2. Rao, B. R., W. Kunysz, R. Fante, and K. McDonald, *GPS/GNSS Antennas*, Artech House, Norwood, MA, 2012.
3. De Lorenzo, D. S., "Navigation accuracy and interference rejection for GPS adaptive antenna arrays," Ph.D. Dissertation, Dept. Aeronaut. & Astronaut., Stanford Univ., Stanford, CA, 2007.
4. Svendsen, A. S. and I. J. Gupta, "The effect of mutual coupling on the nulling performance of adaptive antennas," *IEEE Antennas Propag. Mag.*, Vol. 54, No. 3, 17–38, 2012.
5. Zhou, Y. Z., C. C. Chen, and J. L. Volakis, "Single-fed circularly polarized antenna element with reduced coupling for GPS arrays," *IEEE Trans. Antennas Propag.*, Vol. 56, No. 5, 1469–1472, 2008.
6. Kasemodel, J. A., C. C. Chen, I. J. Gupta, and J. L. Volakis, "Miniature continuous coverage antenna array for GNSS receivers," *IEEE Antennas Wireless Propag. Lett.*, Vol. 7, 592–595, 2008.
7. Chen, M. and C. C. Chen, "A compact dual-band GPS antenna design," *IEEE Antennas Wireless Propag. Lett.*, Vol. 12, 245–249, 2013.

8. Li, J. X., H. Y. Shi, H. Li, and A. X. Zhang, "Design of a 4-element antenna array for BDS anti-jamming applications," *Frequenz.*, Vol. 68, 1–6, 2013.
9. Gao, G., A. Chen, S. Lo, D. Lorenzo, T. Walter, and P. Enge, "Compass-M1 broadcast codes in E2, E5b and E6 frequency bands," *IEEE J. Sel. Topics Signal Process.*, Vol. 3, No. 4, 599–612, 2009.
10. Yang, K. P. and K. L. Wong, "Dual-band circularly-polarized square microstrip antenna," *IEEE Trans. Antennas Propag.*, Vol. 49, No. 3, 377–382, 2001.
11. Balanis, C. A., *Antenna Theory: Analysis and Design*, 3rd Edition, Wiley, New York, NY, 2005.
12. Fante, R. L. and J. J. Vaccaro, "Wideband cancellation of interference in a GPS receive array," *IEEE Trans. Aerosp. Electron. Syst.*, Vol. 36, No. 2, 549–564, 2000.